

Gem News International

Contributing Editors

Emmanuel Fritsch, *University of Nantes, CNRS, Team 6502, Institut des Matériaux Jean Rouxel (IMN), Nantes, France* (fritsch@cnsr-immn.fr)

Gagan Choudhary, *Gem Testing Laboratory, Jaipur, India* (gagan@gjepcindia.com)

Christopher M. Breeding, *GIA, Carlsbad* (christopher.breeding@gia.edu)

COLORED STONES AND ORGANIC MATERIALS

Purplish pink diaspore reportedly from Afghanistan. Diaspore, an orthorhombic aluminum oxide hydroxide mineral with the formula $AlO(OH)$, is a relative newcomer to the jewelry scene, with some stones possessing a captivating ability to change color between pale green, yellow, pink, and purple when viewed in different sources of light (C. Shen and R. Lu, "The color origin of gem diaspore: Correlation to corundum," Winter 2018 *G&G*, pp. 394–403). Here we document a new find of purplish pink gem diaspore reportedly from Nangarhar Province, Afghanistan (figure 1).

Previously, transparent crystals of diaspore in sizes suitable for jewelry purposes were only recovered from mining operations on Ilbir Mountain near the village of Pinarçik,

Figure 1. This purplish pink diaspore is reportedly from a new deposit in Afghanistan, discovered in February 2020. The faceted stones weigh 0.57 to 1.60 ct; courtesy of Donald Hofler. The rough stones range from 4.15 to 17.52 ct; courtesy of Salman Khan. Photo by Diego Sanchez.



Milas District, Muğla Province, Turkey (M. Hatipoğlu and S. Chamberlain, "A gem diaspore occurrence near Pinarçik, Muğla, Turkey," *Rocks & Minerals*, Vol. 86, No. 3, pp. 242–249). Gem diaspore from Turkey has been reported since the late 1970s (K. Scarratt, "Faceted diaspore," *Journal of Gemmology*, Vol. 17, No. 3, 1980, pp. 145–148), but it was not until commercial mining began in 2005 that a consistent supply became available and was subsequently marketed under various trade names including Zultanite and Csarite (S. Kotlowski and L. Rosen, "A short history of diaspore and its trade names Zultanite and Csarite," *International Gem Society*, www.gemsociety.org/article/short-history-diaspore-trade-names-zultanite-csarite). Additionally, alluvial deposits in Myanmar near Mong Hsu have yielded limited amounts of chromium-colored gem-quality crystals in small sizes since 2004 (U Hla Kyi and K.K. Win, "A new deposit of gem quality colour-change diaspore from Mōng Hsu, Myanmar," *Australian Gemmologist*, Vol. 22, No. 4, pp. 169–170).

Dealers Salman Khan (ARSAA Gems & Minerals) and Noshad (Noshad Gems Enterprises), both based in Peshawar, Pakistan, reported that in March 2020, a purplish pink diaspore from a new deposit had reached the gem market. The new material was reportedly coming from the Goshta district of Nangarhar Province near the village of Ragha. The authors obtained several samples from Salman Khan and Donald Hofler, a gem dealer in Texas, to perform gemological and advanced testing to characterize this material. These samples would be classified as F-type samples (collected in the international market) according to the classi-

Editors' note: Interested contributors should send information and illustrations to Stuart Overlin at soverlin@gia.edu or GIA, The Robert Mouawad Campus, 5345 Armada Drive, Carlsbad, CA 92008.

GEMS & GEMOLOGY, VOL. 56, NO. 2, PP. 298–316.

© 2020 Gemological Institute of America

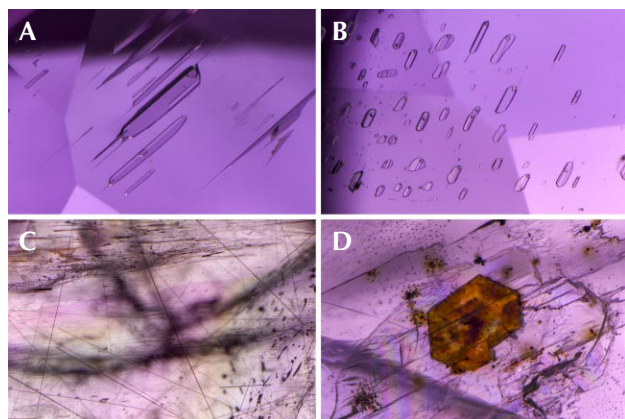


Figure 2. Microscopic examination of the diaspore revealed numerous elongate fluid inclusions (A) and planes of fluid inclusions (B). Also observed in two rough samples were fine black rutile needles (C), and one stone contained an unidentified brown hexagonal crystal (D). Photomicrographs by Nathan Renfro; field of view 1.88 mm (A), 1.44 mm (B), 4.47 mm (C), and 1.41 mm (D).

fication scheme used by GIA's field gemology department (W. Vertriest et al., "Field gemology: Building a research collection and understanding the development of gem deposits," Winter 2019 *G&G*, pp. 490–511). It was also reported by the Peshawar-based dealers that preliminary experiments with gamma irradiation resulted in samples becoming an undesirable dark brownish orange color, but this was not tested further by the authors.

Microscopic examination showed that the dominant type of micro feature in the material is fluid inclusions, typically consisting of a gas bubble, liquid, and occasionally a solid phase. Fine curved black rutile needles were also observed in two of the samples (confirmed by Raman analysis), while one diaspore crystal contained a brown hexagonal crystal that the authors were unable to identify (figure 2). Brown epigenetic staining and cleavage cracks were observed in several samples. Strong doubling by birefringence was also characteristic of the material.

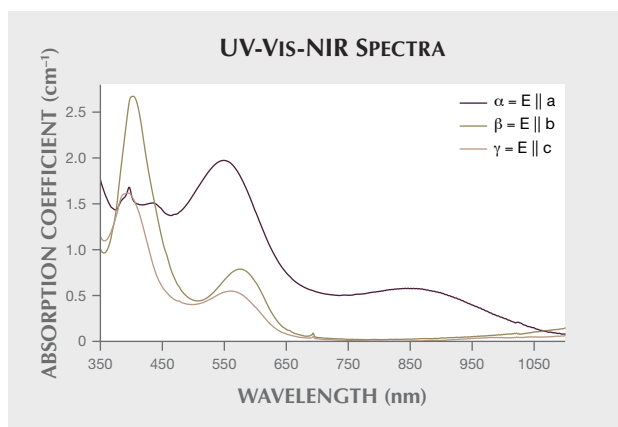
Gemological testing revealed a biaxial positive mineral with refractive indices of $n_{\alpha} = 1.700$, $n_{\beta} = 1.721$, and $n_{\gamma} = 1.749$, and a specific gravity of 3.38. The maximum birefringence observed was 0.049. Examination with a dichroscope showed three distinct pleochroic colors, consistent with a biaxial mineral: dark purplish pink, pale yellow, and pale pink. The diaspore showed a very weak red fluorescence under long-wave ultraviolet light and an irregular chalky yellow fluorescence reaction under short-wave UV. When the samples were examined with daylight-equivalent illumination and compared to incandescent illumination, a slight color shift was observed. The samples appeared less purplish, going from purplish pink in daylight-equivalent lighting to a nearly pure pink hue in

candescent lighting, but no distinct color change of the dominant hue was observed in the faceted samples.

Advanced spectroscopic instrumentation was used to further characterize the new diaspore material. One sample was optically oriented into a polished cube with parallel faces polished perpendicular to the crystallographic axes (T. Thomas et al., "Device and method of optically orienting biaxial crystals for sample preparation," *Review of Scientific Instruments*, Vol. 85, No. 9, 2014, 093105). The ultraviolet/visible/near-infrared (UV-Vis-NIR) absorption spectra of the polished cube revealed broad absorption bands centered in the range of 560 and 580 nm for alpha, beta, and gamma polarizations (figure 3). Under daylight-equivalent lighting, the saturated purple-pink color was consistent with the alpha vibration direction, pale greenish yellow for the beta direction, and light purplish pink for the gamma direction. Under incandescent light, the pleochroic colors were saturated purple-pink for the alpha color, orange-pink for the beta color, and light pink for the gamma color. Color swatches were calculated using the measured spectra to produce a representative color for each pleochroic color and also to show how the colors mix relative to their crystallographic axes (figure 4).

Observations under the microscope showed the cleavage direction in the faceted stones to be nearly parallel to the table (it is inclined slightly, presumably to avoid cleaving when polishing the table facet). This orientation places the b-axis approximately perpendicular to the table facet, which will facilitate the best color face-up, composed primarily of a mixture of the alpha and gamma rays.

Figure 3. UV-Vis-NIR spectra were collected from an optically oriented sample to resolve the alpha, beta, and gamma vibrational directions in the Afghan diaspore. All three spectra showed a broad absorption band centered between 560 and 580 nm resulting primarily from vanadium and chromium. In this sample, the average concentrations were 57 ppma vanadium, 20 ppma chromium, 205 ppma iron, and 84 ppma titanium.



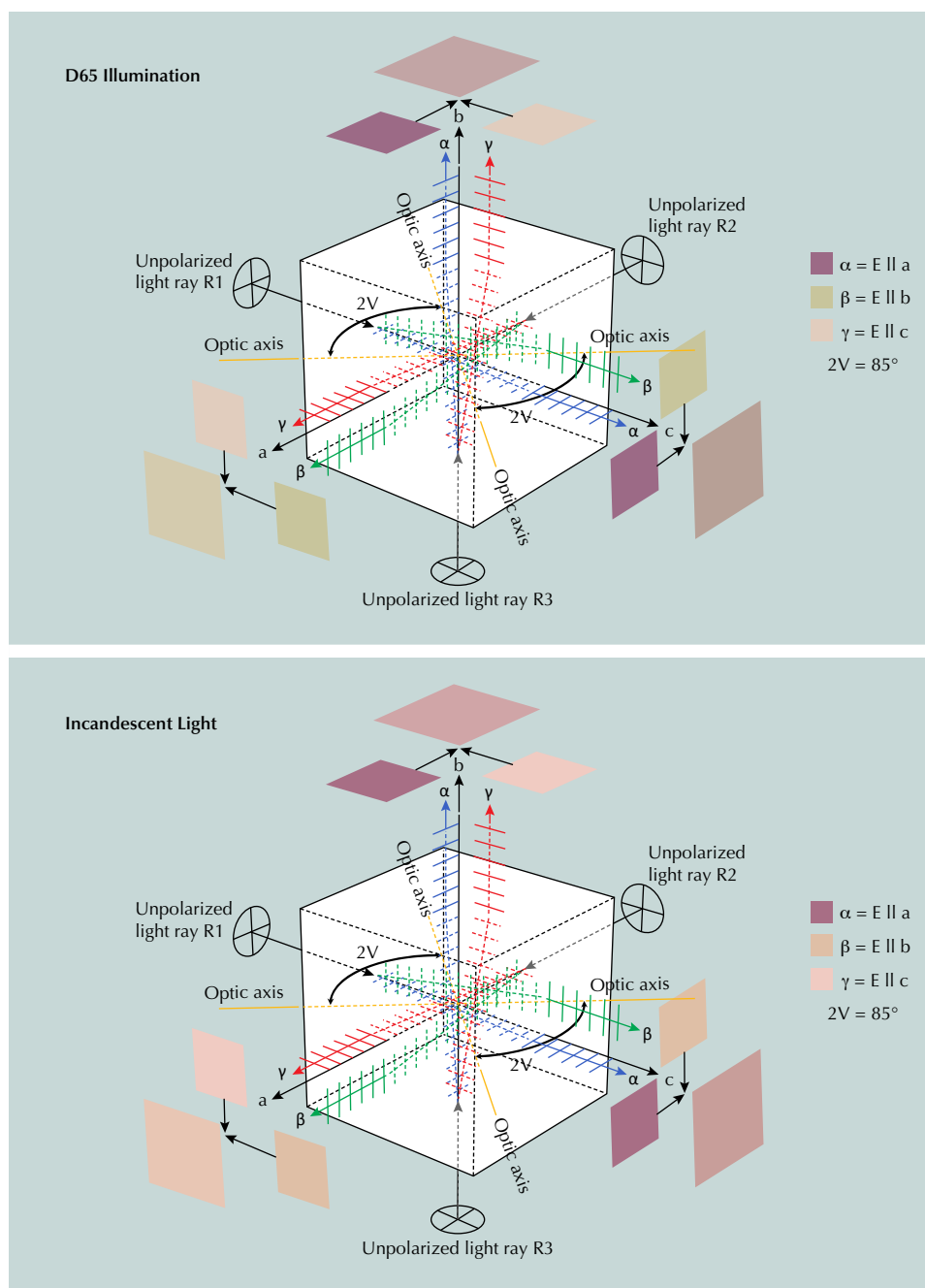


Figure 4. One diaspore sample was fabricated into a crystallographically oriented block in order to measure the polarized spectra, which were used to analyze the color. This figure shows the relationship of the polarized spectra measured parallel to each crystal axis and the resulting colors produced when the polarized spectra are mixed together under daylight (top) and incandescent (bottom) conditions, which is what the viewer would observe using unpolarized light transmitted through the sample normal to a 1 cm path length. Under daylight-equivalent lighting, the alpha color was saturated purple-pink, the beta color was light greenish yellow, and the gamma color was light pink. Under incandescent light, the alpha color was a saturated purple-pink, the beta color was orange-pink, and the gamma color was light pink. The acute $2V$ angle, or angle between the two optic axes, was measured as 85° in this sample. Both axes lie in the optic plane that is perpendicular to the b crystal axis.

Raman analysis confirmed the material's identity as diaspore (figure 5, left). Fourier-transform infrared (FTIR) spectroscopy showed absorption features at approximately 2115 and 1990 cm^{-1} and broad absorption bands at approximately 4080 and 3000 cm^{-1} , all of which are consistent with diaspore (figure 5, right). Chemical analysis of seven samples showed a bulk composition consistent with that of diaspore, and average notable trace element concentrations showed 27 ppma chromium (ranging from 14 to 48 ppma), 31 ppma vanadium (from 14 to 59 ppma), 213 ppma titanium (from 67 to 428 ppma), and 252 ppma iron (from 137 to 350 ppma).

This exciting discovery of purplish pink diaspore from Afghanistan may prove to be a significant new deposit. While production volume is currently unknown, several kilograms of material have been reported and large faceted stones of nearly 50 ct have been described on social media (Mark Smith, @thailankagems). The color of this diaspore can be attributed mainly to trace element concentrations of chromium and vanadium. The concentrations of these elements are generally different from those in Turkish diaspore, which has significantly lower vanadium, and those in Burmese material, which

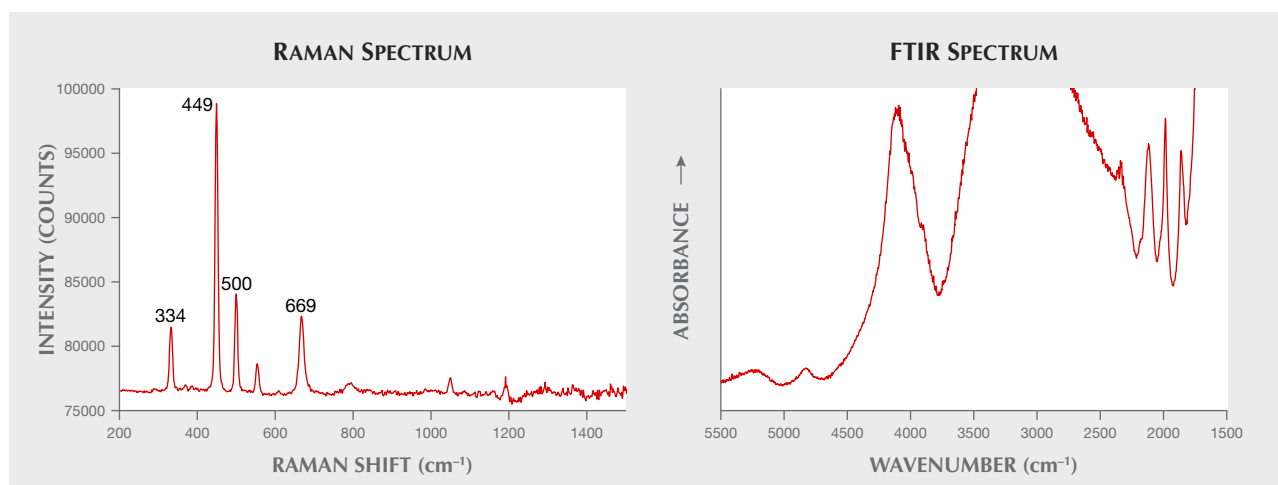


Figure 5. The purplish pink gem material from Afghanistan showed a Raman spectrum (left) that matched diaspore, with a dominant peak at 449 cm^{-1} and smaller peaks at 334 , 500 , and 669 cm^{-1} . Its FTIR spectrum (right) was consistent with diaspore, with absorption features at approximately 2115 and 1990 cm^{-1} and broad absorption bands at approximately 4080 and 3000 cm^{-1} .

generally has much higher chromium. This new attractive color of gem-quality diaspore will certainly be a welcome addition to the gem trade.

Ian Nicastro
San Diego, California
Wim Vertriest
GIA, Bangkok

Nathan Renfro, Ziyin Sun, Aaron Palke, and Paul Mattlin
GIA, Carlsbad

Fossil ivory update with Lee Downey. Lee Downey, owner of Artifactual (Tucson, Arizona), spoke with us in early 2020 about his 35 years in the fossil ivory carving trade and the impact of ivory bans on his business. Until recently Downey carved fossil ivory from mammoth and walrus tusks thousands of years old; he has never used elephant

ivory. But legislative measures banning all ivory in response to the poaching of African elephants have diminished ivory demand.

Downey got his start in silver and turquoise and established Artifactual in the late seventies. Since then, he has lived and worked in an ivory carving village in Bali with artisans he calls “the most talented carvers in the world.” When he first arrived in Bali, they were carving bone and coconut shell. His task was to carve animals and animal skulls out of fossil ivory. “We created a trade,” he said. He showed us two of Artifactual’s current offerings (figure 6). “But now the material has become flat-out illegal in eight states.”

Since 2014, California, Hawaii, Illinois, Nevada, New Hampshire, New Jersey, New York, and the District of Columbia have enacted prohibitions against trade in ivory. (Two other states, Oregon and Washington, have banned



Figure 6. Fossil walrus ivory carvings by Artifactual. The base of the octopus carving is chalcosiderite. Photos by Kevin Schumacher.



Figure 7. A mammoth tusk carved with sea life by Lee Downey. Photo by Kevin Schumacher.

only ivory from living elephants.) Downey said that Hawaii's ban in particular "tanked" the trade. Customers even in states where ivory remains legal are reluctant to purchase fossil ivory, he said.

"I understand why they're doing it," Downey told us. "I'd rather save all wildlife if there was a way." But he said the effect of the bans on his business has forced him to prepare to exit the fossil ivory trade. He is selling his current ivory inventory at lower prices and not buying additional material.

Downey showed us a mammoth tusk carved with sea life (figure 7) as well as two belt buckles featuring mammoth ivory (figure 8). All of them use material sourced from Alaska. "This washes up on beaches and comes out of gold mines," he said. "It's highly sought after by the knife makers. It's got colors that elephant ivories will



Figure 8. A selection from Artifactual's inventory of fossil ivory. Clockwise from top left: belt buckle with mammoth ivory, knife with mammoth tooth handle, belt buckle with mammoth ivory, and frog carving of fossil walrus ivory. Photo by Kevin Schumacher.

never have. It just keeps weathering out of the dirt." Downey added that this ivory is at least 10,000 years old.

Mammoth ivory can be differentiated from elephant ivory by a simple field test to observe its natural grain lines. But there is no test to determine whether a specimen of walrus ivory comes from a fossil or a modern animal. According to Downey, this is a problem in the trade.

Artifactual uses fossil walrus ivory from St. Lawrence Island, Alaska. This ivory is 500 to 15,000 years old and dug by the native Yupik people. "It's part of their income, and they own the island," he said. "For us it's a legitimate and ethical trade."

Downey added that the legislation on ivory also prohibits mammoth tooth because it comes from an ivory-bearing animal. He showed us a knife with a carved mammoth tooth handle (figure 8). Knife makers are some of the biggest buyers of mammoth tooth, he said, and the bans have dramatically impacted their business.

As a result of the decreased demand for ivory, Artifactual is moving its business to other materials, including jet, natural American turquoise and variscite, steel (figure 9, left), and meteorite. "Gaia" (figure 9, right) is carved from a piece of the Gibeon iron-nickel meteorite, which landed in prehistoric times in Namibia and is believed to be around four billion years old. The company also does a lot of business in silver.

Downey has also sought out materials similar to ivory but without the ethical and legal challenges. He has begun



Figure 9. Left: “Alpha,” a stainless steel foundry-cast skull by Artifactual, one of six in a series. Right: “Gaia,” the second skull Downey carved from a piece of the Gibeon meteorite, has a tridymite crystal inclusion in the forehead. The geometric pattern on its surface was caused by the slow process of cooling as the meteor moved through space. Photos by Kevin Schumacher.

carving moose antlers naturally shed by the animals (figure 10). “The moose antler has been a really good substitute

Figure 10. A moose antler carving of a horned toad by Lee Downey. Photo by Duncan Pay.



for the ivory,” he said. He also recently began carving vintage billiard balls. “We’ll carve anything that’s carvable,” he said.

For our video interview with Lee Downey, visit <https://www.gia.edu/gems-gemology/summer-2020-gem-news-fossil-ivory-update>.

Erin Hogarth and Duncan Pay
GIA, Carlsbad

The “Fragility of the Eternal” kunzite: Origin, cutting, and identification. Lapidary, the art of colored stone fashioning, is an art that requires a keen eye, talent, and great patience. Different gem materials have their particular quirks that must be considered when planning the various steps required to reach the ultimate goal of obtaining the most aesthetic stone while usually also optimizing weight yield.

Spodumene is known to challenge even the most experienced cutter owing to its high fragility, perfect cleavage planes, and unpredictability in different cutting directions. This is further magnified when the rough is exceptionally large and the cutter’s goal is to produce the largest faceted kunzite in the world.

This was author VT’s aim as he prepared to work on a piece of rough spodumene that weighed 2,950 g. The untreated crystal (figure 11) originated from Kunar Province in Afghanistan. Although a wide crack was visible at one end and about 30% of the opposite end contained numerous inclusions, the removal of both sections still left more than 1.5 kg of relatively clean rough after 20 hours of wire sawing (the safest method under the circumstances). Since the rough was oversized, some of the routine cutting ac-



Figure 11. The pronounced pleochroism of the rough spodumene crystal weighing 2,950 grams, seen here in two orientations, was one of the properties that had to be considered during fashioning. Photos by Arjuna Irsutti.

cessories such as dops and transfer holders, as well as the cutting tactics, had to be adapted for the job.

Prior to the start of the process came the design element. No journey can be completed without knowing the destination, and so rather than playing it safe and opting for a simple design, the artist, VT, chose a truly challenging facet pattern of his own design that incorporated 914 facets. The “Fragility of the Eternal” design is based on the stained glass window of the iconic Notre Dame cathedral in Paris. The stone is the fifth in a series of six cut designs that fall under VT’s “World Heritage” project.

VT would also have to revise his usual strategy due to the size. So instead of cutting the pavilion first, followed by the girdle, crown, and finally the table facet, it was necessary to start with the table facet for this masterpiece. This presented its own challenges since the faceting required specialized equipment belonging to a friend in Moscow. The choice of equipment was also dictated by the material’s fragility and perfect cleavage, which prevented the use of coarse laps. This combined to make the work time-consuming, especially since large facets were the order of the day.

The next step required the rough to be rounded in order to achieve the basic outline of the stone in its face-up position. This meant that sufficient pressure had to be applied to the 1.5 kg preform using both hands. Eventually the correct shape resulted. The diameter measured approximately 85 mm, while the table facet came in at 65 mm. This allowed the final weight to be approximated using formulas and the facet plan shown in figure 12. The result, between 2,500 and 3,000 ct, indicated that it would supersede the largest known faceted spodumene, an 1,800 ct green spodumene cut by John Sinkankas in 1959 that was destined for the Royal Ontario Museum in Toronto.

Although the rest of the preforming could not be done traditionally by hand, VT managed to use his faceting unit

with custom-made dops provided by his friend and former student Danial Hu. The pre-faceting step took considerable time to complete because the goal was to create an important piece of art and each facet needed to be cut in a pattern that matched the stained glass window in the Notre Dame cathedral with a precision of tenths of a millimeter. Perhaps the most complex part of the process was creating 16 mains and 16 additional lines extending from the center (culet) to the girdle, each containing eight (main) and five (additional) parallel-sided facets, continuous with one another. An equally challenging task was ensuring the proportions were correct while cutting 18 rows of facets of different sizes and shapes, where one often does not depend on another, and finally making the last row of facets correspond exactly with the girdle, which was already pre-shaped. It was impossible to change the width of the final facets without breaking the pattern, which meant that the pavilion had to finish precisely where the girdle started. In other words, the width of all 18 rows had to be exactly proportional to the diagram. Another look at figure 12 is enough to show that the girdle does not simply separate the crown from pavilion as in traditional faceted stones: It is an essential element of the design.

Many chances for something to go awry existed during the cutting process. Only a slight error in judgment or calculation would result in disaster. For example, if the rows of facets were just a bit too wide, there would not have been enough space for the design and the pavilion would have required a complete recut. If some were too narrow, the girdle would have needed recutting, resulting in a smaller stone, which would also have meant recutting the table facet. Fortunately, the final facet positions aligned perfectly around the girdle, and the stone’s final diameter (83.7 mm) was off by just over 1.0 mm from the initial calculations.

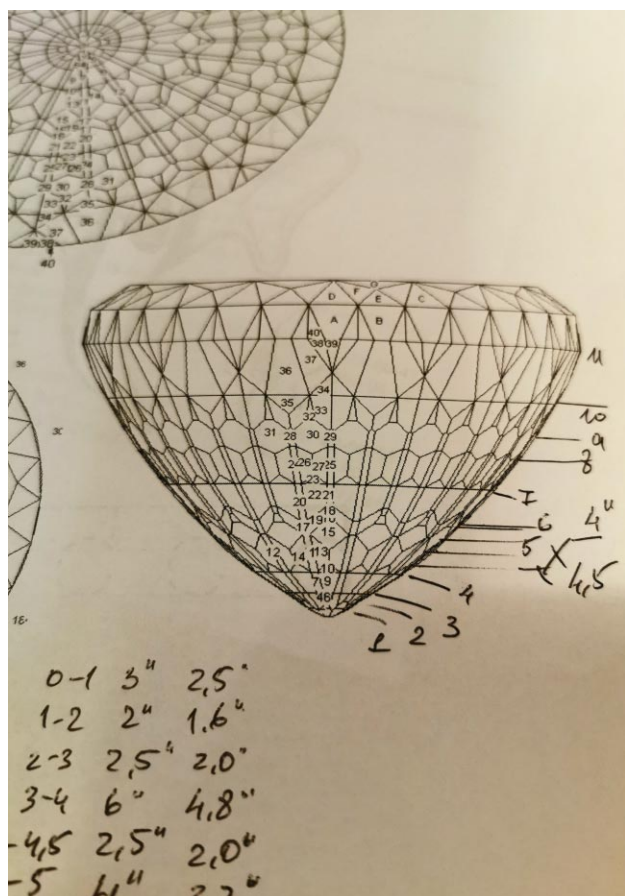


Figure 12. A working diagram showing the facet positions. These helped estimate the final weight of the finished stone before work began on the rough. Photo by Victor Tuzlukov.

The next steps, pre-polishing and polishing of the pavilion facets (figure 13), were straightforward in comparison. Yet, as mentioned previously, the sheer size meant that the vertical pressure had to be applied equally over the whole stone during pre-polishing, requiring modification of the technique used for routine work on smaller stones. If too much force was applied to the left or right side, or back and forth, the facets would become too large and the pattern would be broken. To overcome this, the stone's own weight provided sufficient force on the rotating lap so that the pressure was always equally distributed.

After more than two months of daily work, the pavilion was polished. The next step was transferring the stone to a new dop to polish the crown. Unlike traditional lapidary procedures, directly heating the stone as part of the transfer was not an option, as the process could crack the stone along the twin plane in the direction it needed to be dopped, and because the size was once again a factor when it came to how evenly the heat warmed the stone. This resulted in the application of a technique that the late Jeff Ford from Michigan shared with VT in 2006, using a com-

ination of wax and superglue. The wax is placed on the hot dop, which is softened by the heat. The cold stone is then placed, pavilion first, in contact with the wax, and an impression of the surface is made in it. One drop of superglue is enough to secure the stone firmly in position, and it can be removed by reapplying a little heat to warm the wax again.

After three months of work, the final polishing step was completed. The gem's removal from the dop was an exciting moment, and it was wonderful to finally see the end product in all its glory (figure 14). The finished piece weighed 3,051 ct, very close to the maximum estimated weight of 3,000 ct.

The final step in the stone's journey was its submission to GIA's Bangkok laboratory for examination and a report. The gemologists were excited to study such a large kunzite, although the size, 83.75–83.79 × 65.00 mm, presented challenges that limited the testing equipment that could be used. Hence, basic gemological techniques came to the fore, with Raman spectroscopy the only advanced technique used as a final confirmation. The stone was found to be anisotropic with a loupe and microscopic observation

Figure 13. The polishing step on the stone's pavilion begins to show the intricate optical effects of the completed piece. Photo by Victor Tuzlukov.





Figure 14. The 3,051 ct “Fragility of the Eternal,” containing 914 facets, is believed to be the world’s largest cut kunzite. Photo by Adisorn Wattananich.

up to 70× magnification, and this property was also apparent in terms of the strong pleochroism that could be easily seen as the stone was turned. The same purple and green colors are also clearly evident in figure 11.

The RI readings of 1.660–1.676 (birefringence of 0.016) together with the trichroic colors seen through a dichroscope showed it was optically biaxial. Inclusions such as growth tubes, transparent crystals, negative crystal fingerprints, and a “natural” retained on the girdle all proved the stone was natural. Combined with the weak and moderate orange zoned long-wave ultraviolet fluorescence reaction, the data were consistent with spodumene, kunzite variety.

Since the stone was cut and submitted by VT with a series of photographs documenting this fact, the GIA report (dated May 27, 2020) also mentioned that it was represented as cut by him. Since it was the largest known faceted kunzite examined by GIA at the time, and indeed the largest faceted example of its kind known to exist, a GIA Notable Letter was issued to accompany the report.

Victor Tuzlukov
Bangkok

Patcharee Kaewchaijaroenkit and Nicholas Sturman
GIA, Bangkok

Occurrence of petrified woods in the Russian Far East: Gemology and origin. Petrified woods are used all over the world as an excellent material for souvenirs, jewelry, and spectacular collectible pieces. A new occurrence of petrified wood was discovered in 2014 in the Primorsky Krai region of the Russian Far East, near the village of Kiparisovo. The fossils were found in the northwestern part of a sand and gravel quarry, at the contact of rhyolitic volcanic ash tuffs and basalts overlapping them. The sample sizes varied from several centimeters to two meters.



Figure 15. Marble polar bear with silver fish on a petrified opalized wood stand. Photo by Svetlana Kulenko; courtesy of Anton Akulenko.

Local jewelers started using the wood fossils as stands for souvenirs (figure 15) and polished collectible samples. The petrified wood appeared in regional jewelry stores and attracted Chinese tourists’ attention, creating demand for the raw material from China’s market.

More than a hundred samples were studied at the Analytical Center of the Far Eastern Geological Institute of the Far Eastern Branch of the Russian Academy of Sciences (FEGI FEB RAS). We examined the mineral composition, structure, and gemological characteristics using standard gemological equipment, a Nikon E100 POL optical microscope, and a MiniFlex2 X-ray diffractometer (XRD). Several examples of petrified wood were found: white, yellowish, marble-like, chalcedony-like, banded, banded chalcedony-

Figure 16. Cabochons of petrified wood from the Russian Far East. Photo by Dmitrii G. Fedoseev.



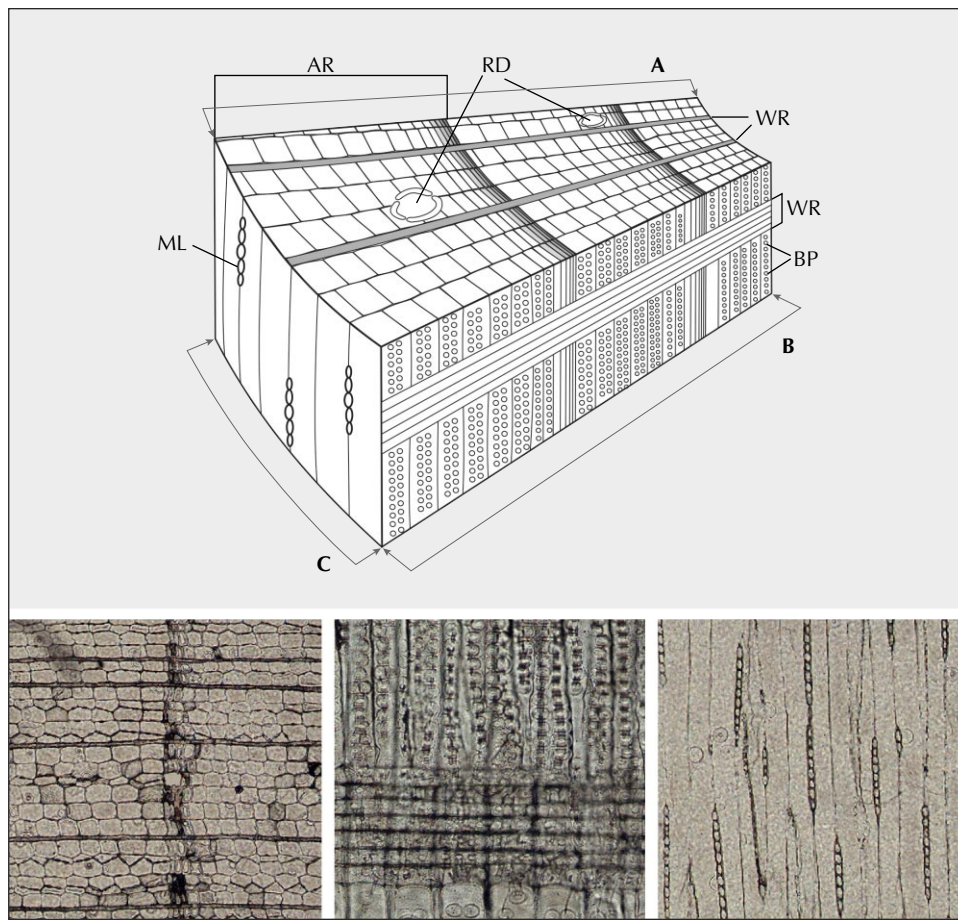


Figure 17. Top: Schematic cross section of a conifer's trunk showing the transection (A), radial section (B), tangential section (C), annual ring (AR), resin ducts (RD), wood rays (WR), bordered pits (BP), and middle lamellae (ML). Bottom left: Transection of petrified wood with wood rays (horizontal lines), resin ducts, and annual ring; field of view 5.5 mm. Bottom center: Radial section of petrified wood with wood rays (horizontal lines) and tracheids with bordered pits (round-shaped); field of view 2.7 mm. Bottom right: Tangential section of petrified wood with chains of middle lamellae; field of view 5.5 mm. Photomicrographs by Dmitrii G. Fedoseev.

like with brownish growth rings, partially carbonized, and black coalified (figure 16).

The refractive indices of polished plates ranged from 1.40 to 1.54 in different areas and corresponded to chalcedony, opal, and quartz. Luminescence was weak bluish or greenish under short-wave UV; most samples were inert under long-wave UV. Samples had a fibrous cellular structure. The shape of the cells (tracheids) was angular, rectangular, and sometimes subsquare (figure 17, bottom left). The transections of the samples showed very narrow single-row horizontal wood rays. Vertical resin ducts that looked like white dots were located in the latewood area of the annual rings (vertical dark band) (figure 17, bottom left). On the radial sections of the samples, we observed wood rays (horizontal lines) and bordered pits (round-shaped pores) (figure 17, bottom center). Middle lamellae (chains-like cells) were seen on a tangential section of petrified wood (figure 17, bottom right).

The absence of vessels, the unique type of wood rays and tracheids with bordered pits, the character of the middle lamellae, and the presence of vertical resin ducts indicated that these samples belonged to coniferous plants. X-ray diffraction analysis showed that all the varieties of petrified wood had an opal-cristobalite-tridymite composition.

The geology of the area allowed us to imagine the formation conditions. As a result of catastrophic volcanic eruptions of rhyolitic magmas as glowing ash clouds, and late effusions of mantle magmas, thick layers of volcanic ash and overlapping basalt flows were formed. The basalt lava flows outpoured into the water basin with a temperature exceeding 1000°C. Lavas overlapped the flooded trunks and thick bottom sediments of ash silts. When the basalt melt came into contact with water, the surface of the lava flow instantly quenched with the formation of pillow lavas. The space between the pillow lavas was filled with clastic glassy rocks known as hyaloclastites.

Thus, the flooded trees were under the hyaloclastites and pillow lavas. Some trees, under the weight of a lava flow, had taken a vertical position. Some trunks that sunk in hyaloclasts were charred, while trunks in ash silts remained unchanged. During silicification, the charred parts of the trunks acquired a black color and the uncharred parts became white, light yellow, to brownish (figure 18). Buried trees underwent strong deformation with flattening of the trunks, splitting, and fragmentation of wood.

The main source of silica when replacing the cells of trees by quartz or opal was ash silts. This was promoted by a low-alkaline water-saturated volcanic ash with a high SiO₂ content (over 72 wt.%). The silicon-containing



Figure 18. Left: Part of a petrified wood. Right: Opalized petrified wood sample with play-of-color. Photos by Dmitrii G. Fedoseev.

aqueous solutions penetrated woods that, under anaerobic conditions, represented local geochemical barriers where precipitation of free silica replacing plant cells occurred. Depending on the concentration of silicon in the solution in plant cells, the deposition of opal, chalcedony, or quartz occurred. The foregoing description allows us to imagine a majestic picture of how Nature created this wonderful combination of the worlds of plants and stones.

Vera Pakhomova, Valentina Solyanik, Dmitrii Fedoseev,
Svetlana Y. Kulenko (s_buravleva@yahoo.com), and
Vitaliya B. Tishkina
Far East Geological Institute (FEGI FEB RAS)
Vladivostok, Russia
Valeriya S. Gusarova
Far Eastern Federal University (FEFU), Vladivostok

Portrait of a Paraíba rough: Challenging gems in hard times. The impact of COVID-19 on the global gem trade is unquestionable. Traditional sales and services in most consuming countries came to a grinding halt. But the effects of lockdowns are also deeply felt in distant trade centers that rely on a steady supply of rough gemstones to feed their cutting, treating, and manufacturing industries.

Many of the brokers that take care of the transfer from producing countries to manufacturing hubs were

suddenly unable to perform their vital role in the gemstone supply chain. Without a constant flow of new rough material, the wheels that drive the entire industry stop turning.

When a crisis like this happens, people are forced to turn to other sources. In the trading center of Chanthaburi, Thailand, the most obvious source of rough is easily overlooked: the back of the safe. Over the years, rough parcels of varying qualities have been kept for a rainy day, and in some cases material has been held back for years to keep prices buoyant via artificial scarcity.

Difficult times have seen many established businesses releasing some of these old parcels, sometimes of material not seen in volume for years (or even decades), such as Kenyan rubies from the John Saul mine or spessartine “Fanta” garnet from Nigeria.

Both authors had the privilege to handle one of the unique pieces that came from the back of someone’s safe into the market.

When SBL first saw this piece, his immediate reaction was that it was tanzanite. Several other colleagues and knowledgeable friends had the same first impression. It was difficult to imagine the true identity of this crystal, which was the size of a duck’s egg.

This was an 85 g, 427 ct piece of unheated cuprian or Paraíba-type tourmaline rough from Mozambique (figure 19; see also the video at www.gia.edu/gems-gemology/summer-

Figure 19. This 85 g Mozambican cuprian tourmaline was released in the Chanthaburi market in May 2020. While everyone can agree that this is a unique and valuable piece, there is no agreement on the price that can be put on it. Photo by Simon Bruce-Lockhart.



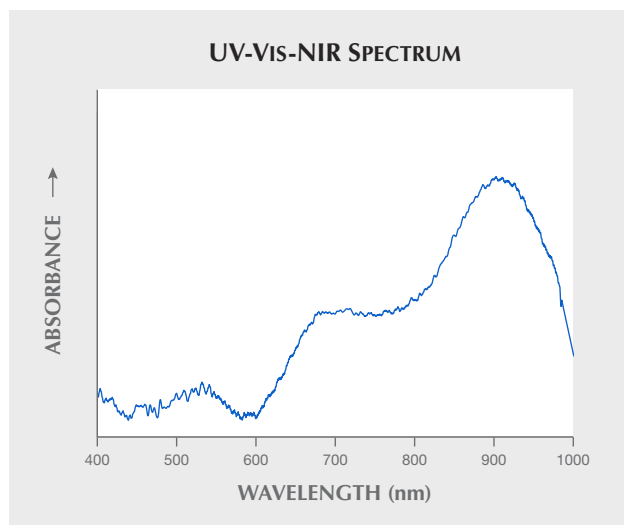


Figure 20. The UV-Vis-NIR spectrum shows clear absorption peaks at 660 and 900 nm that are typical for cuprian tourmaline.

2020-gemnews-mozambique-paraiba-rough). The stone was shown in the rough gem trading circuit of Chanthaburi near the end of May 2020. The GIA laboratory in Bangkok was able to do some limited testing on the stone, confirming that it was indeed a cuprian tourmaline (figure 20).

Large crystals of copper-bearing tourmaline were seen a decade ago at the advent of the Mavuco mines, but nothing of this size and quality has been seen on the open market for some time. For more on this material, see B.M. Laurs et al., “Copper-bearing (Paraíba-type) tourmaline from Mozambique,” Spring 2008 *G&G*, pp. 4–30.

There is little doubt that such a large, prestigious piece attracts attention. After that, the consensus stops. While it is undeniable that this stone is very valuable, no one can agree on precisely how valuable it is.

The decisions of how to heat and cut it to open up that coveted blue-green color produced by copper are critical to the value-adding process. The results of heat treating Mozambican cuprian tourmaline can be seen in figure 22 of Laurs et al. (2008).

The unheated Paraíba gem was taken to the handful of factories in Chanthaburi and Bangkok capable of buying and value-adding such a piece. Factoring in cracks, internal stress, and the orientation of some inclusions, all the factories determined that the stone should be cut into several pieces.

But everyone had a different opinion of exactly how to manufacture this piece. And this is where the dreams of Paraíba profits get smashed on the anvil of market reality.

A well-saturated large crystal will, when cut into numerous smaller pieces, exhibit a paler saturation of the original hue. Given that the market will pay much more per carat for larger Paraibas of intense color than for smaller paler Paraibas, the range of potential value outcomes regarding the number of pieces to cut is dizzying.

Furthermore, heat treatment of any stone is unpredictable, but tourmaline is a notoriously fickle gem to heat. Would you simply remove the frosted surface and heat it before sawing and preforming? This carries the risk that the gem will shatter uncontrollably during heating, but also the possibility of producing a single Paraíba tourmaline of spectacular size and a coveted deeper color. Or would you play it safe by cutting and grinding it into several smaller preforms and heating the many pieces? This mitigates some of the risks, but sacrifices the potential for capitalizing on the size of the rough.

Even if you play it safe, there is still no guarantee that minor unintended cracking will not require the resizing and re-orientating of preforms before faceting, which could significantly reduce the final color and weight yet again.

The transformative yet risky process of slicing, preforming, heating, and faceting is in some ways a gamble. The reality is that neither buyer nor vendor actually knows what will happen, and there is an element of chance layered on top of the manufacturer’s skill. The coveted “Paraíba” hue and saturation after heating are not guaranteed, and cases of “overcooking” cuprian tourmalines until only a pale pink color remains are not unheard of. These many variables create unknowable outcomes.

The most prudent buyers calculate their offers based on the risk of as many as six or more paler pieces, and offer much lower than expected when seeing this magnificent piece of rough. The vendors optimistically hold to their dream of a higher value based upon two or three larger, well-saturated pieces—and with such a wide disparity in value-outcome consensus, rough gems like this take time to sell. In the case of this piece, no agreement was reached after several rounds of back-and-forth between the different parties, and the stone was returned to its owner.

While this story is not unique, it highlights many aspects of the gem trade that most people throughout the supply chain are unfamiliar with. In these tough COVID times, it becomes especially important to realize how many hands have handled the gems we are seeing and which challenges every single one faces.

*Simon Bruce-Lockhart
Chanthaburi, Thailand*

*Wim Vertriest
GIA, Bangkok*

A new deposit of pink natrolite from Indonesia. In early 2020, a parcel of stones representing some unique material found in early 2020 from the island of Nusa Kambangan, Central Java, Indonesia, was sent to Taiwan Union Lab of Gem Research (TULAB) for certification service. At the beginning, wholesalers claimed that the gemstone was thomsonite. Because its texture was very similar to the green-blue pectolite variety Larimar produced in the Dominican Republic, the stone was also misrepresented with the trade name “pink Larimar.”



Figure 21. Rough stones and polished cabochons of pink natrolite. The heart-shaped cabochon is 35.6 mm wide. Photo by Yu-Ho Li.

By observing the rough stones with host rocks provided by the supplier, the occurrence was found to be vein-filling or cavity-filling within basalt. These stones had orange-pink to brownish pink color with white zoning and showed a botryoidal or radial crystal habit (figure 21).

The average specific gravity of this parcel of gemstones was 2.24, and the spot RI was 1.49. With the owner's consent, the parcel of polycrystalline material was tested with a Vickers hardness tester. The values were converted to Mohs hardness and ranged from 4.4 to 4.6. The samples' Raman spectra were analyzed and compared to the RRUFF mineral spectral database; unexpectedly, the results were consistent with published

spectra of natrolite ($\text{Na}_2\text{Al}_2\text{Si}_3\text{O}_{10}\cdot 2\text{H}_2\text{O}$) instead of thomsonite ($\text{NaCa}_2\text{Al}_5\text{Si}_5\text{O}_{20}\cdot 6\text{H}_2\text{O}$) (figure 22). The UV-Vis spectra revealed that the pink natrolite stones had a wide absorption band at 400–570 nm (figure 23). The EDXRF results also indicated that the pink gemstone was natrolite and contained a trace iron component. On the basis of EDXRF and UV-Vis results, the orange-pink to brownish pink color appeared to have been caused by Fe^{3+} ; however, this presumption still needs further verification.

This natrolite from Indonesia has a unique rose pink color and Larimar-like texture on polished surfaces, which is not common in natrolite from other localities. Although initially misrepresented by the merchant as thomsonite or

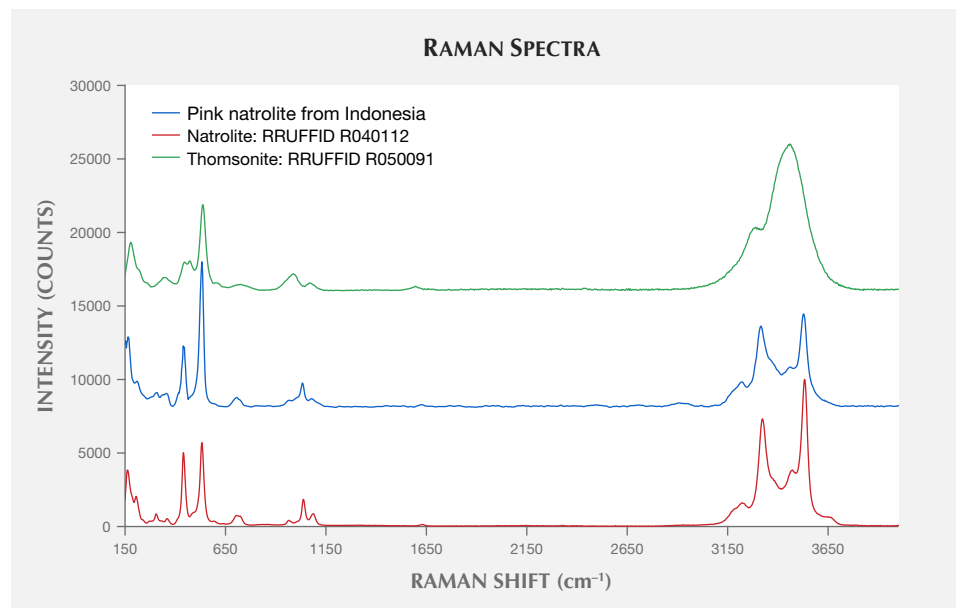


Figure 22. Stacked Raman spectra of the pink natrolite from Indonesia compared to those of natrolite and thomsonite published in the RRUFF database; all spectra are normalized and baseline corrected.

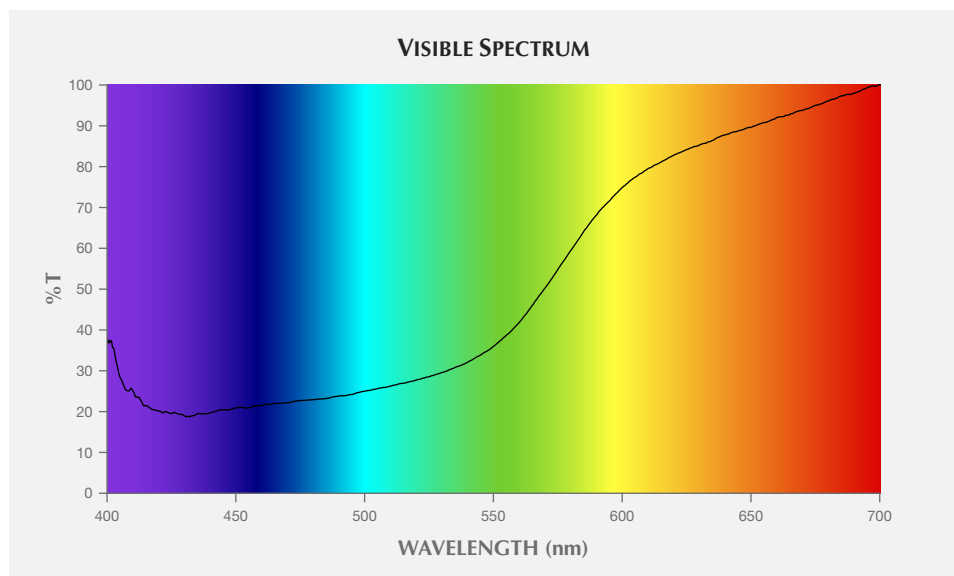


Figure 23. The normalized visible-light transmission spectrum of pink natrolite shows a wide absorption band at 400–570 nm that results in a brownish pink to orange-pink color.

pink Larimar, its beautiful appearance and durability are indeed comparable to Larimar. Subsequently, a new trade name “rhodatroilite,” meaning “rose natrolite,” was developed by the merchant for marketing this gemstone because of its color and texture. With enough mine production, pink natrolite from Indonesia has the potential to become a popular gemstone on the market.

Yu-Ho Li

*Institute of Earth Sciences
National Taiwan Ocean University, Keelung*

Huei-Fen Chen

*Institute of Earth Sciences and
Center of Excellence for Oceans
National Taiwan Ocean University*

Shu-Hong Lin

*Institute of Earth Sciences
National Taiwan Ocean University
Taiwan Union Lab of Gem Research, Taipei*

DIAMONDS

Finders, keepers: Field trip to Crater of Diamonds, USA.

There’s only one place on earth where the general public can prospect for diamonds directly from a primary kimberlite pipe: Crater of Diamonds State Park. This park is nestled among the pines, 100 miles off the interstate near the town of Murfreesboro, Arkansas. It boasts a network of scenic walking trails, picnic sites, and campsites. At its Diamond Discovery Center, visitors can learn about the local geology. Staff are also on hand to identify any minerals that are taken home, per their “finders, keepers” policy. The park is an ideal spot for a field trip. The state also hosts many other unusual igneous rocks, including carbonatite, lamprophyre, and lamproite. With this in mind, our university petrology class piled into a van to visit Arkansas

and learn about mantle-derived magmas and associated volcanism. As a side quest, we wanted to try prospecting.

The park’s main attraction is diamonds, but there are also olivine, pyrope, almandine, and amethyst to be found. Most of the diamonds recovered there are small (approximately 0.20 ct or less); see figure 24. Rarely, prospectors have found stones larger than 1 carat, including the famous Uncle Sam, a whopping 40.23 ct. The park’s diamond-bearing rocks are comprised of hypabyssal olivine lamproite and phlogopite-rich tuffs and breccias, characterized by

Figure 24. These diamonds from Crater of Diamonds State Park were mined previously by other prospectors. They range up to approximately 0.06 ct. Photo by Roy Bassoo.





Figure 25. Prospecting for diamonds at the Mauney mine, now Crater of Diamonds State Park, circa 1908. Photo courtesy of the Crater of Diamonds Archives.

high Mg# values (atomic ratio of Mg to Fe in an igneous rock) and K_2O content (E. Walker, "Petrogenesis of the Prairie Creek, Arkansas, diamondiferous olivine lamproite," PhD thesis, University of Western Ontario, Ontario, Canada, 1991). The deposit grades between 0.01 and 1.25 carats per 100 tons (D.P. Dunn, "Xenolith mineralogy and geology of the Prairie Creek lamproite province, Arkansas," PhD thesis, University of Texas, Austin, 2002). In the early twentieth century, when the richest material was mined, there was a brief diamond rush in the area (figure

25). After a string of ownership changes and failed business ventures, visions of a South African-style diamond district never materialized. In 1972 the state of Arkansas purchased the land and opened it to public prospecting. Since then, visitors have found more than 33,000 diamonds (www.arkansasstateparks.com).

After a couple of days learning about the igneous rocks in the area, it was time to test our luck at treasure hunting. We gathered buckets, shovels, and sieves from park headquarters for a small rental fee and headed out to 15 hectares

Figure 26. A local prospector digging for diamond ore and demonstrating sieving technique. Photos courtesy of Glenn Worthington.





Figure 27. Three of the diamonds the authors collected from Crater of Diamonds State Park (approximately 0.01–0.05 ct). Note the irregular and fragmented morphology and brown to yellow colors. Photos by Roy Bassoo.

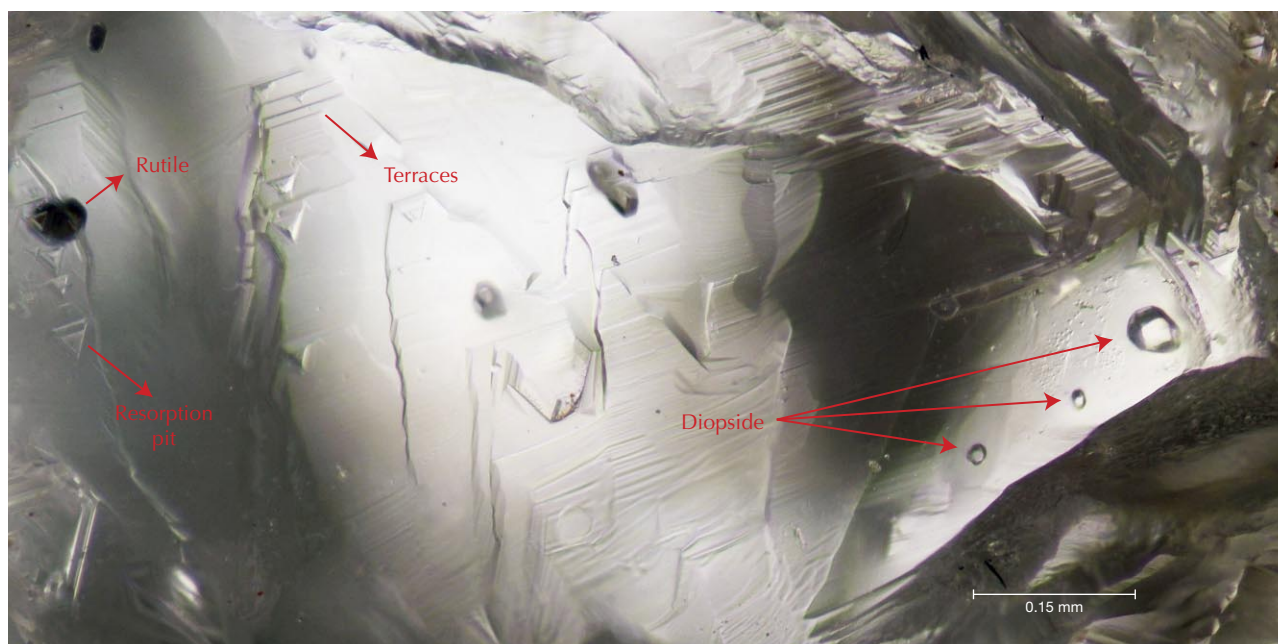
of routinely plowed “blue ground.” We chose a spot, shoveled soil into buckets, and carried these heavy parcels of dirt to the wash station for sieving (figure 26). The trick is to shake the sieve back and forth just beneath the water in the horizontal plane, then rotate and repeat. This motion should concentrate the heavy minerals in the center and bottom of the sieve. Then, like a master chef, the prospector flips the entire mineral concentrate upside down and examines the heavies that sink to the bottom.

In three hours, we found a small collection of diamonds! Granted, they were also very small in size, ranging from 0.01 to 0.05 ct (figure 27). Most prospectors at Crater of Diamonds miss stones this small, but as trained mineralogists we were attentive to small crystals. The diamonds were predominantly colorless, although a couple were yellow to brown. Their dominant morphology was

octahedral with uncommon dodecahedrons and macles. Resorption pits and terraced surfaces were pervasive. The diamonds were also fragmented, likely due to the explosive nature of the diatreme crater.

Treasure in hand, we then turned to the science. Back in our lab, we ground and polished the diamonds into wafers to examine their composition and crystal interiors. Raman spectroscopy determined that inclusions of rutile and diopside were common (figure 28). N contents, measured with Fourier-transform infrared spectroscopy, ranged from trace amounts (type IIa) to 1250 ppm (type IaAB). Cathodoluminescence imagery showed blue to turquoise response colors, typical of diamonds mined from primary deposits worldwide. They also feature fascinating patterns of growth banding and resorption truncations, which indicate a complex mantle crystallization history (figure 29).

Figure 28. Terraced dissolution surface textures and inclusions of rutile and diopside embedded within the diamond. The diopside inclusions are aligned along a growth band. Photomicrograph by Roy Bassoo.



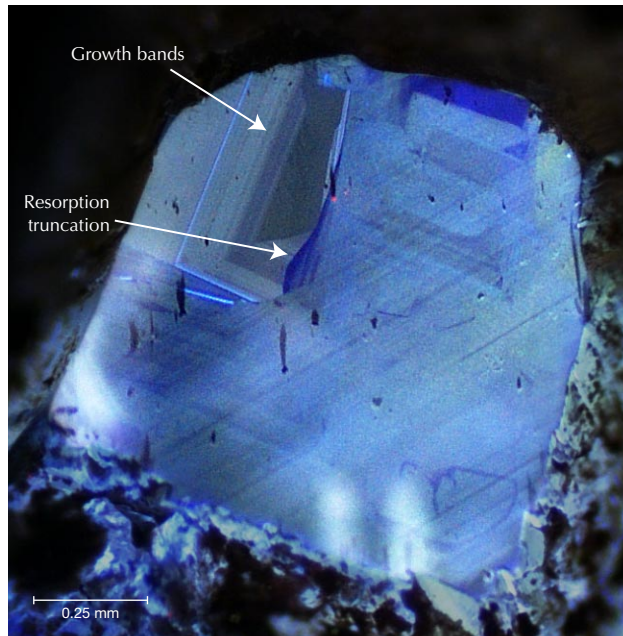


Figure 29. Cathodoluminescence image of a polished diamond wafer, showing complex banding and truncations that highlight different diamond growth conditions. Image by Roy Bassoo.

We found Crater of Diamonds to be a thoroughly enjoyable treasure hunting adventure. Our visit gave us hands-on experience with diamond-bearing igneous rocks and challenged us to imagine how diamonds formed beneath the North American craton. We have new appreciation for the back-aching labor required by the artisanal miners worldwide who are the foundation of the gem trade. Scientific understanding and trade awareness were the substance of our visit, highlighted by moments of joyful discovery. We encourage readers to put Crater of Diamonds State Park on their gemology “bucket list” to hunt for their very own American diamond.

Roy Bassoo and Kenneth S. Befus
Department of Geosciences, Baylor University
Waco, Texas

SYNTHETICS AND SIMULANTS

Greenish blue glass imitating gem silica. Gem silica, also known as “chrysocolla chalcedony,” is considered the most valuable variety of chalcedony. Its attractive blue to bluish green color is generated by finely disseminated minute inclusions of chrysocolla. The main sources include Taiwan, the United States, Mexico, Peru, and Indonesia. For years, gem silica has been especially popular in Taiwan. Due to the pleasing saturated blue color of Taiwanese material, which is among the world’s finest, it commands a premium price.

At the same time, the current lack of production in Taiwan is driving prices substantially higher. Thus, imitations and treatments are gradually emerging in the marketplace, confusing customers. Recently we obtained three polished specimens from a gift shop in Taidong County, Taiwan (near the locality of the gem silica mine), that appeared to have good quality of color and transparency (figure 30). The merchant claimed they were gem silica mined in Taiwan, but they were subsequently identified as glass imitations.

Standard gemological tests showed the following properties of the three samples: color—uniform greenish blue; diaphaneity—translucent; spot RI—1.48; SG—2.48 to approximately 2.57; fluorescence—inert to long-wave UV radiation, weak greenish white to short-wave UV radiation. Actual gem silica, meanwhile, has the following properties: color—commonly uneven; spot RI—1.54; SG—approximately 2.63. Examination with a gemological microscope revealed numerous obvious gas bubbles of different sizes (figure 31, left). In the case of the marquise sample, numerous gas bubbles led to a relatively low specific gravity. When viewed with oblique incident light, many small dimples were visible on the polished surface (figure 31, right). In addition, there were some small conchoidal fractures along the bottom edges of samples. In order to gain a more thorough understanding, further advanced analysis was carried out.

FTIR reflectance spectroscopy showed a main reflected band at approximately 1065 cm^{-1} (figure 32), consistent with the characteristic spectrum of glass (see Fall 2019 GNI, p. 443–445; T.B. Wang et al., “Relationship between the frequency of the main LO mode of silica glass and angle of incidence,” *Journal of Chemical Physics*, Vol. 119, No. 1, 2003, pp. 505–508). Chemical analysis by LA-ICP-MS detected multiple elements: Si (averaging 617000 ppmw), Na (averaging 151000 ppmw), Al (averaging 101000 ppmw), Ca (averaging 24900 ppmw), K (averaging 19600 ppmw), Ba (aver-

Figure 30. Two oval and one marquise cabochon of greenish blue glass samples ranging from 2.17 to 2.60 ct. Photo by Min Ye.



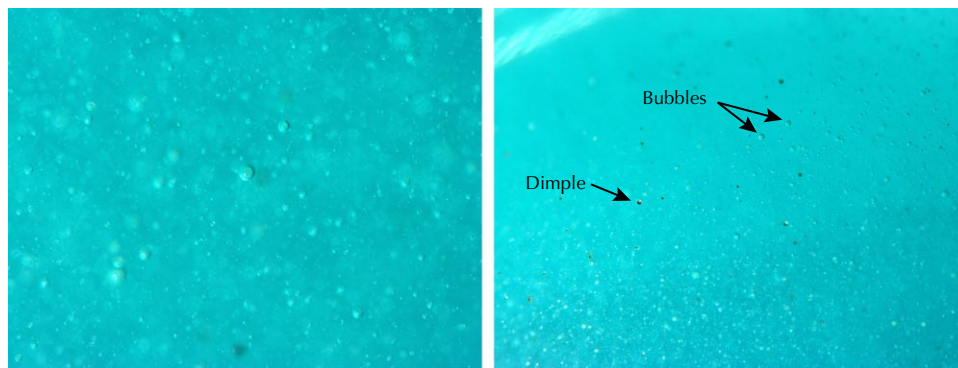
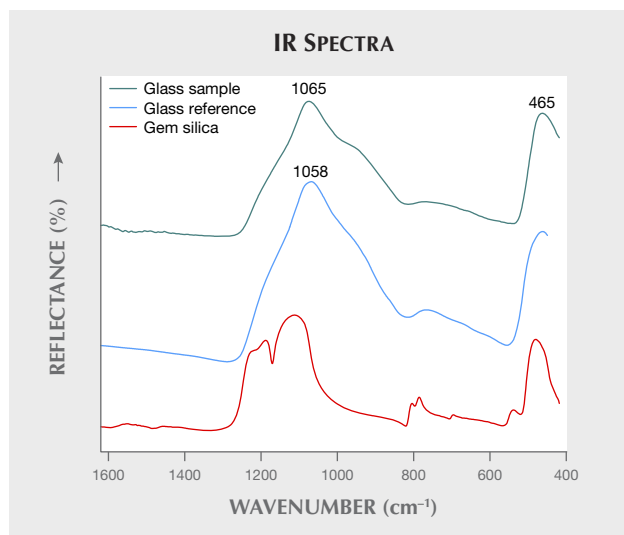


Figure 31. Left: Numerous gas bubbles of various sizes were typical internal features of the three samples; field of view 1.28 mm. Right: Many small dimples could be found on the polished surface; field of view 3.70 mm. Photomicrographs by Min Ye in overhead lighting (left) and oblique illumination (right).

aging 17800 ppmw), Pb (averaging 3840 ppmw), Mg (averaging 2580 ppmw), Fe (averaging 1620 ppmw), Cu (averaging 5940 ppmw), and Cr (averaging 716 ppmw). This composition identified the three samples as silicate glass, which is decidedly different from gem silica (whose majority component is silica and chrysocolla, a copper silicate). UV-Vis-NIR spectra of the specimens presented a strong broad absorption band around 760 nm (figure 33), revealing Cu^{2+} as the coloring agent. In addition, two weak absorption bands at 424 and 439 nm might have been related to trace amounts of Fe^{3+} , while the 690 nm band was possibly due to the existence of Cr^{3+} (see W. Thiemson et al., "Redox ratio and optical absorption of polyvalent ions in industrial glasses," *Bulletin of Materials Science*, Vol. 30, 2007, pp. 487–495; V. Vercamer, "Spectroscopic and structural properties of iron in silicate glasses," PhD thesis, Université Pierre et Marie Curie-Paris VI, 2016, pp. 97–145).

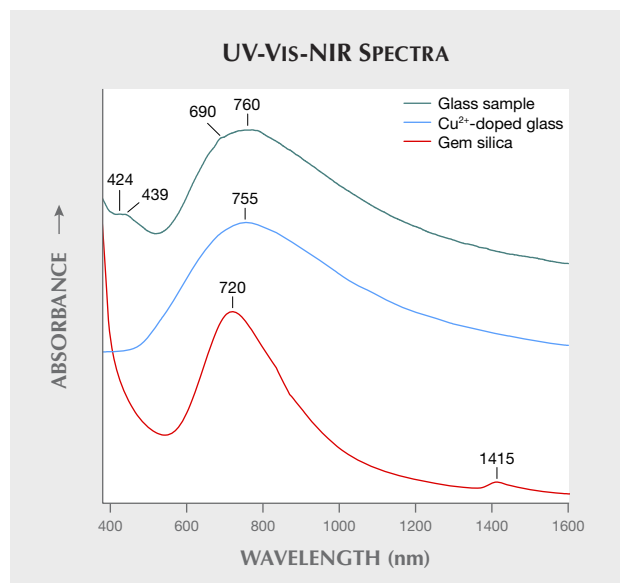
Figure 32. Representative infrared reflectance spectra of the three samples (green trace) were compared with the reference spectra for glass (blue trace) and natural gem silica (red trace, collected by the author). The diagnostic reflected peak of the glass sample is near 1065 cm^{-1} , quite different from the gem silica peaks. The spectra are offset for clarity.



Combining all the evidence, the three greenish blue samples were confirmed to be artificial glass colored by an unknown copper additive. Gas bubble inclusions were the diagnostic feature for identification, and FTIR spectra were also helpful. This case is a reminder that customers need to be cautious when purchasing gemstones, even near the geographic source.

Min Ye and Andy H. Shen (shenxt@cug.edu.cn)
Gemmological Institute
China University of Geosciences, Wuhan

Figure 33. Typical UV-Vis-NIR absorption spectra of the three samples (green trace) were compared with those of Cu^{2+} -doped glass (blue trace) and natural greenish blue gem silica (red trace, collected by the author). In the typical plot for the glass samples, the absorption band around 760 nm is assigned to Cu^{2+} . Two weak absorption bands in the glass imitation at 424 and 439 nm might be related to trace amounts of iron, while the 690 nm band is possibly due to the presence of chromium. The spectra are offset for clarity.



Marble imitation of jadeite rough. In recent decades, jadeite prices have risen dramatically. Driven by profit, a variety of imitations are found in the jadeite jewelry market. Meanwhile, imitations such as quartzite are fixtures in the rough jadeite market. Recently, our research group received for testing a 30 kg stone that resembled jadeite rough and was submitted as such. The stone had a yellow weathered skin with a grainy texture, similar to jadeite. There was a narrow “window” (figure 34) that showed the green color of the material underneath the skin. For identification purposes, the authors exposed another area on the surface of the rough and then ground it for testing.

Due to the weight, some standard gemological testing methods could not be used, such as measurement of refractive index and specific gravity. Therefore, the sample was studied by visual and 10× loupe observation, hard-

Figure 34. This 30 kg stone was submitted as a piece of jadeite rough. A narrow window (in the red circle) opened on the surface of the rough reveals a green material underneath the skin. Photo by Huang Jing.



Figure 35. The newly exposed part of the rough stone was identified as marble. Photo by Huang Jing.

ness testing, chemical reagent detection, and infrared spectroscopy.

Scratch testing revealed a Mohs hardness between 2 and 5, lower than jadeite’s hardness of 6–7. The surface was yellow, just like the weathered skin of jadeite rough, and the narrow window in figure 34 revealed green color below the skin. Scrubbing the window with alcohol removed the green color, indicating that the window had been dyed. To test the material, diluted hydrochloric acid was dropped on the newly exposed portion in figure 35. The acid foamed continuously, showing that the sample contained carbonate (Z. Hanli et al., “Study on acid polishing of carbonate white jade,” *Journal of Gems and Gemmology*, Vol. 5, No. 4, 2003, pp. 24–27). The acid testing combined with visible observations and hardness testing identified the sample as marble. The jadeite granular structure came from the marble’s cleavage planes.

Testing of the exposed part by infrared spectrometry revealed 1525, 1432, 1080, 883, 670, 553, and 483 cm^{-1} absorbance peaks, characteristic of serpentinized marble.

The serpentinized marble’s yellow weathered skin and grainy texture could have easily been mistaken for jadeite rough. This serves as an alert to the industry to be careful even when examining rough, as imitations are showing up.

Huang Jing, Yan Shuyu, and Chen Shuxiang (corresponding author, kedachenshuxiang@163.com)

School of Materials Science and Engineering

Qilu University of Technology
(Shandong Academy of Sciences)

Shandong, China

Cheng Youfa
National Gold and Diamond Testing Centre of China
Shandong